International Journal of Food Science +Technology

Institute of Food Science +Technology ifst

International Journal of Food Science and Technology 2024, **59**, 7971–7986

Original article

Development of chitosan nanoparticle loaded with *Tricholoma fracticum* extract and evaluation of *in vitro* antioxidant activity

Fadime Canbolat,[1]* İsmail Acar[2] & Ruhiye Nilay Tezel[3,4]

1 Department of Pharmacy Services, Vocational School of Health Services, Çanakkale Onsekiz Mart University, 17020 Çanakkale, Turkey
2 Department of Organic Agriculture, Başkale Vocational High School, Van Yuzuncu Yıl University, 65080 Van, Turkey
3 Department of Chemistry, Polymer Synthesis and Analysis Laboratory, Çanakkale Onsekiz Mart University, 17020 Çanakkale, Turkey
4 Department of Chemistry and Chemical Processing Technologies, Lapseki Vocational School, Çanakkale Onsekiz Mart University, 17800 Çanakkale, Turkey

(Received 16 August 2024; Accepted in revised form 26 August 2024)

Summary The objective of this study was to develop *Tricholoma fracticum* extract-loaded chitosan nanoparticles (TFNPs) by ionic gelation method and to evaluate their *in vitro* antioxidant activity. Phenolic and flavonoid contents in the *T. fracticum* extract were measured spectrophotometrically and chromatographically. Characterisation of NPs was evaluated by field emission scanning electron microscopy (FE-SEM), transmission electron microscopy (TEM), ZETA analysis, Fourier-transform infrared spectroscopy (FT-IR), UV–visible spectroscopy (UV–Vis) and thermogravimetric analysis (TGA). *In vitro* antioxidant capacity was determined using 2,2-diphenyl-1-picrylhydrazyl (DPPH) and 2,2′-azino-bis(3-ethylbenzothiazoline-6-sulfonic acid) (ABTS) assays. The phenolic and flavonoid contents in the *T. fracticum* extract were measured as 7.1 ± 0.3 mg Gallic Acid Equivalent/g extract and 5.5 ± 0.6 mg Quercetin Equivalent/g extract, respectively. The particle size, polydispersity index (PDI) and zeta potential of Blank NP1 and TFNP were 265.5 ± 15.8 nm, 0.4, 38.7 ± 4.0 mV and 333.2 ± 16.3 nm, 0.4, 37.0 ± 4.1 mV, respectively. The highest antioxidant activity was observed in TFNP, followed by *T. fracticum* extract, chitosan and blank NP, respectively. The preserved or enhanced antioxidant activity observed in the encapsulated *T. fracticum* extract indicates the potential for loading similar mushroom extracts onto chitosan and thus preserving their bioactive properties.

Keywords Antioxidant, characterisation, chitosan nanoparticle, chromatography, ionic gelation, *Tricholoma fracticum*.

Introduction

Mushrooms, consumed as foodstuffs since ancient times, are among the remarkable foods with pharmacological properties (Tel *et al*., 2012; Altıntas, 2023). Many studies have reported that edible mushrooms contain amino acids, fatty acids (mostly unsaturated or polyunsaturated such as oleic, linoleic and linolenic acids), phenolic and flavonoid compounds, vitamins such as thiamine, riboflavin, ascorbic acid, ergosterol and niacin, sterols and some essential minerals such as phosphorus and iron (Sánchez, 2010; Thu *et al*., 2020; Acar *et al*., 2021; Alkin *et al*., 2021; Bal, 2021; Kumar *et al*., 2021). Mushrooms containing lectins, polysaccharides, polysaccharide-peptide and polysaccharide-protein complexes, lanosten-type triterpenoids, as well as phenolic and flavonoid compounds exhibit anticancer, antioxidant, radical scavenging, antibacterial, antifungal and anti-inflammatory properties (Sánchez, 2010; Tel *et al*., 2012; Kumar *et al*., 2021; Altıntas, 2023) The fact that edible mushrooms can be obtained at low cost and are biocompatible makes their use in the field of health widespread (Yavuz & Gul, 2022).

Tricholoma species, which can be obtained cheaply, predominantly consist of edible mushroom species (Allı & Şen, 2016). The pharmacological effects of these mushroom species have garnered significant interest from researchers (Tel *et al*., 2012). *Tricholoma fracticum*, a member of the *Tricholoma* family, is a fungus species that lives symbiotically with trees, typically found under coniferous trees such as pine and fir. It is widespread in temperate regions, mainly in Anatolia, Europe and North America (Qonitah *et al*., 2023). Recently, *T. fracticum* has attracted scientific attention; however, there is limited information regarding its bioactive components and pharmacological properties in the literature. It is an edible mushroom with a bitter taste profile (Allı & Şen, 2016). The use of edible mushrooms to enhance health benefits is becoming increasingly common in the pharmaceutical

*Correspondent: E-mail: fadime.canbolat@comu.edu.tr

doi:10.1111/ijfs.17585

field. Nevertheless, mushrooms, containing approximately 90% water and 10% dry matter, have a short shelf life and start to decompose rapidly (Sánchez, 2010; Kartal *et al*., 2022). Overcoming the disadvantages of taste and stability of edible mushrooms and increasing their potential efficacy require new approaches. In this context, researchers are interested in developing nanoparticles (NPs) in nanotechnology. Numerous bioactive compounds are being formulated into NPs, leveraging the progress in this field.

The use of chitosan in the development of NPs is considered as an important and widely accepted strategy worldwide (Aljebory & Alsalman, 2017; Morin-Crini *et al*., 2019; Gao & Wu, 2022). Chitosan, a natural polysaccharide, is the hydrolysis product of chitin, is recognised as an effective component in NP formulations (Sandeep *et al*., 2013; Acay *et al*., 2022). In NP form, chitosan's high surface area and reactive functional groups allow for the efficient loading of bioactive compounds. Additionally, its biological compatibility enables NPs to be safely metabolised by the human body (Canbolat *et al*., 2024). Studies have reported that chitosan can prolong shelf life and stabilise foods by inhibiting degradation through its antimicrobial properties (Morin-Crini *et al*., 2019; Karimirad *et al*., 2020; Valizadeh *et al*., 2021; Gao & Wu, 2022). Chitosan is thought to positively affect the stabilisation of mushrooms and shelf life of mushrooms. Studies by Karimirad *et al*. (2020) and Valizadeh *et al*. (2021) reported that the essential oil-loaded chitosan NPs positively effect mushroom shelf life (Karimirad *et al*., 2020; Valizadeh *et al*., 2021).

This study aimed to develop chitosan NPs loaded with mushroom extracts to demonstrate the applicability of mushrooms in various formulations and to utilise their bioactive substances. In the study, *T. fracticum* extract was loaded onto chitosan using the ionic gelation method to develop a novel NP. The morphology, size and structural content of the developed NPs were characterised using Field emission scanning electron microscopy (FE-SEM), Transmission electron microscopy (TEM), ZETA particle size and potential analysis, Fourier-transform infrared spectroscopy (FT-IR), UV–Visible spectroscopy (UV–Vis) and thermogravimetric analysis (TGA). *In vitro* antioxidant capacity was assessed through 2,2-diphenyl-1-picrylhydrazyl (DPPH) and 2,2′-azino-bis(3-ethylbenzothiazoline-6-sulfonic acid) (ABTS) antioxidant activity analyses.

Materials and methods

Mushroom materials

The fruiting bodies of *T. fracticum* were collected in Çanakkale province in 2023, as detailed below. The samples collected in the field were transported to Çanakkale Onsekiz Mart University Polymer Laboratory (Turkey) on the same day.

Specimen examined: Around the Safiye Hüseyin Elbi Girls' Dormitory, under *Pinus* sp. trees, 40° 06′42″ N, 26° 25′55″ E, 214 m, 20.12.2023, collector no: Acar 1563. Dr. Ismail Acar from Van Yüzüncü Yıl University retained selected specimens within the fungarium for preservation as voucher specimens. Fresh mushroom samples were properly cleaned from all kinds of dust and contaminants. Then, the mushrooms were placed on blotting paper and air-dried at room temperature (22 ± 2 °C) out of the light.

Chemicals

To prepare the chitosan solution, 5 mg of chitosan (CAS: 9012-76-4), derived from shrimp shells (medium molecular weight, ≥75% deacetylated), was purchased from Sigma Aldrich (Darmstadt, Germany). Sodium tripolyphosphate (STPP) (CAS: 7758-29-4) was also obtained from Sigma Aldrich (Darmstadt, Germany). Additionally, 2,2-Azino-bis(3-ethylbenzothiazoline-6-sulfonic acid) (ABTS), 1,1-Diphenyl-2-picrylhydrazyl (DPPH), ascorbic acid, gallic acid (GA) and trolox (6-hydroxy-2,5,8-tetramethylchroman-2-carboxylic acid), Folin–Ciocalteu Reagent (2 N), methanol (HPLC grade), ethanol (HPLC grade), aluminium chloride (anhydrous, powder, 99.999% trace metals basis), sodium nitrite (≥99.0%) and sodium carbonate (≥99.5%) were purchased from Sigma Aldrich (Darmstadt, Germany).

Preparation of *Tricholoma fracticum* extract

The *T. fracticum* extract in ethanol was obtained using the method described by Dhamodharan & Mirunalini (2013). In summary, *T. fracticum* was ground into powder (50 g) and mixed with 500 mL of ethanol (30 °C) for 24 h at 150 rpm. The resulting extract was filtered through Whatman No. 4 filter paper. Subsequently, ethanol was removed using an evaporator at 40 °C, and the remaining residue was dried at room temperature in the dark. The dried residue (340 mg) was then dissolved and enriched in ethanol (10 mg mL^{-1}). The extract was stored at 4 °C for analysis.

Analysis of phenolic and flavonoid compounds in *Tricholoma fracticum* extract

Phenolic compound analysis

The phenolic compounds in *T. fracticum* extract were determined using the Folin–Ciocalteu reagent. This determination was equivalent to GA using the method described by Slinkard & Singleton (1977). 0.2 N Folin–Ciocalteu reagent was prepared from the originally purchased Folin–Ciocalteu solution of 2.0 N by diluting at

a volume ratio of 1:10. A 7.5% (w/v) sodium carbonate solution was prepared by dissolving 7.5 grams of sodium carbonate in 100 mL of distilled water (Akdeniz *et al*., 2021). Then, 50 µL of 1000 µg mL^{-1} mushroom extract and GA solutions at five different concentrations (3.78 µg mL^{-1}, 7.56 µg mL^{-1}, 15.13 µg mL^{-1}, 31.25 µg mL^{-1}, 62.5 µg mL^{-1} in methanol) were taken. Subsequently, 950 µL of distilled water was added to each sample. Finally, 250 µL of 0.2 N Folin–Ciocalteu reagent was mixed into each sample in 2 mL eppendorf tubes.

After incubation at room temperature for 3 min, 750 µL of 7.5% sodium carbonate solution was added to complete the reaction, which was then allowed to mature at room temperature for 2 h. At the end of this time, following this period, the absorbance values of the mushroom samples and standards were determined using a JASCO V-650 spectrophotometer (JASCO, Japan) at a wavelength of 765 nm. Within the scope of the study, each sample and standard were analysed in triplicate, and the mean values were used. The total phenolic content of the samples was calculated as mg Gallic Acid Equivalent (GAE)/1 g of extract (Akdeniz *et al*., 2021).

Flavonoid analysis

The total flavonoid content in the *T. fracticum* extract was determined based on the study conducted by Barros *et al*. (2007). Quercetin (QE) was used as the reference standard. To establish a calibration curve, various concentrations of QE in ethanol were prepared, resulting final calibration standard concentrations of QE 2.5 µg mL^{-1}, 5 µg mL^{-1}, 10 µg mL^{-1}, 15 µg mL^{-1} and 20 µg mL^{-1}. From these QE solutions, 100 µL were pipetted and mixed with 640 µL of distilled water. Subsequently, 30 µL of 5% sodium nitrite solution was added and vortexed. After 5 min, 30 µL of 10% aluminium chloride solution (in methanol) was added and vortexed again. After incubating the samples for 1 min, 200 µL of 1.0 M sodium hydroxide was added. For the analysis of mushroom extract, 100 µL of the extract was used instead of the QE reference standard. The samples were then kept in the dark at room temperature for 40 min. Subsequently, the absorbance values of the samples were determined using a JASCO V-650 spectrophotometer (JASCO, Japan) at a wavelength of 515 nm. Within the scope of the study, each sample and standard were analysed in triplicate, and the mean values were used. A calibration curve of absorbance against five concentrations (2.5 µg mL^{-1}, 5 µg mL^{-1}, 10 µg mL^{-1}, 15 µg mL^{-1} and 20 µg mL^{-1}) of QE was plotted. Using this curve, the total flavonoid content in the mushroom extract was calculated as mg QE equivalent per gram of extract (Dursun *et al*., 2024).

Analysis of phenolic compound content using Exactive Plus Orbitrap Liquid Chromatography-tandem mass spectrometry (LC-MS)

In addition to the phenolic compound analysis conducted using the Folin–Ciocalteu reagent on the *T. fracticum* extract, the phenolic compound content was also analysed using the Exactive Plus Orbitrap Liquid Chromatography tandem mass spectrometry (LC-MS) device at the Bingöl University Application and Research Laboratory Center (Bingöl, Turkey). Merck Purosper® STAR RP-18 end capped Hibar® HR model UHPLC column (100 mm × 2.1 mm, 3 µm) was used for chromatographic analysis. The column oven temperature was set at 30 °C. Mobile phase A consisted of a 0.5% acetic acid solution for the gradient system, and mobile phase B consisted of methanol (Ercan, 2024). The sample injection volume was 20.0 µL, and the flow rate was set at 0.3 mL min^{-1}, with a total analysis time of 20 min. Mobile phase A was delivered to the system up to 15.50 min, operating at a flow rate of 100%. Subsequently, from 15.50 to 16 min, mobile phase B was delivered at a flow rate of 98%. After 16 min, mobile phase A was reinstated at 100% flow rate. The Orbitrap High-Resolution Mass Spectrometry (HRMS) equipped with a heated electrospray ionisation interface was operated in both positive (Full MS/AIF) and negative (Full MS/AIF) modes. The ionisation interface had a sheath gas flow rate of 35; auxiliary gas flow rate of 7; spray voltage of 3.5 kV; capillary temperature of 350 °C; auxiliary gas temperature of 350 °C; and S-lens RF level set at 50. MS scanning was performed in the mass range of 60–800 m/z with a resolution of 17 500; ACG target.

A stock standard solution containing 77 phenolic compound standards at concentrations of 10 ng mL^{-1}, 20 ng mL^{-1}, 40 ng mL^{-1}, 60 ng mL^{-1}, 80 ng mL^{-1} and 100 ng mL^{-1} was prepared by diluting the stock standard solution. 50 mg of mushroom extract was weighed into a 15 mL falcon tube, then 10 mL of ethanol was added. The mixture was dissolved in an ultrasonic bath for 20 min and then vortexed for 5 min to facilitate dissolution. Subsequently, centrifugation was conducted at 4500 rpm for 15 min. The supernatant was then filtered through a 0.22 µm pore size, 25 mm diameter Polytetrafluoroethylene (PTFE) syringe filter into a 1.5 mL vial designated for subsequent injection into the analytical instrument. All procedures were executed in triplicate to ensure analytical reproducibility.

Synthesis of blank chitosan nanoparticles (blank NPs)

In our study, chitosan NPs were developed using the commonly preferred ionic gelation method in the literature (Bodnar *et al*., 2005; Zhang *et al*., 2008; Agarwal

et al., 2018; Tzeyung *et al*., 2019; Jardim *et al*., 2022). The ionic gelation method relies on the interaction between positively charged chitosan and negatively charged cross-linker at room temperature. The most commonly used cross-linker in studies is STPP (Canbolat *et al*., 2024). When the basic phase containing STPP (pH 7–9) is added to the acidic phase containing chitosan (pH 4–6), NP formation occurs spontaneously due to the intra- and intermolecular bonds between the positively charged amino groups of chitosan and the negatively charged phosphorus groups of STPP (Zhang *et al*., 2004; Gokce, 2008). It has been reported in the literature that depending on the concentration ratios of chitosan and STPP, clear solutions, cloudy suspensions and aggregates can form. Zhang *et al*. (2004) suggested that the smallest NP size is achievable when the chitosan/STPP ratio is 5-fold (Zhang *et al*., 2004). Therefore, this study initially synthesised two different ratios of chitosan NPs (2-fold and 5-fold, w/w) to delineate an appropriate concentration range. Comparative characterisation of these synthesised blank NPs determined the optimal chitosan/STPP (w/w) ratio, guiding the selection of the preferred method for synthesising *T. fracticum* extract-loaded chitosan NPs (TFNP).

3 mg mL^{-1} chitosan solution prepared with 1.5% acetic acid was stirred for 24 h. Then, the pH was adjusted to 4.5 using 10 N sodium hydroxide. For ionic gelation, STPP was dissolved in distilled water to prepare a 1.5 mg mL^{-1} STPP solution (pH 9.0). Dropwise, 12 mL of the 1.5 mg mL^{-1} STPP solution was added to the 3 mg mL^{-1} chitosan solution (pH 4.5) (Blank NP1; Chitosan/STPP ratio of 2-fold). The solution was stirred at a low speed for 24 h (Gokce, 2008).

To prepare Blank NP2 (Chitosan/STPP ratio 5-fold), 0.6 mg mL^{-1} solution (pH 9.0) of STPP dissolved in distilled water was prepared. Subsequently, 12 mL of the 0.6 mg mL^{-1} STPP solution was added dropwise to the 3 mg mL^{-1} chitosan solution (pH 4.5) (Gokce, 2008). The solution was then stirred at a low speed for 24 h.

All NPs were centrifuged at 8000 rpm for 40 min, and the pellets were stored at +4 °C for characterisation analysis. Wet pellets were used for particle size and zeta potential analysis, while lyophilised pellets were used for other characterisation analyses.

Synthesis of *Tricholoma fracticum* extract-loaded chitosan nanoparticles (TFNP)

The synthesis of TFNP was conducted based on the preferred method determined through characterisation analyses comparing Blank NP1 and Blank NP2 developed at different ratios. The selected method was Blank NP1, with a chitosan/STPP (w/w) ratio of 2, as identified from the characterisation results. Following the protocol described by Dhamodharan & Mirunalini (2013), 12 mL of 1.5 mg mL^{-1} STPP solution and 3 mg mL^{-1} *T. fracticum* ethanol extract were added to a 3 mg mL^{-1} chitosan solution (pH 4.5) (Gokce, 2008; Dhamodharan & Mirunalini, 2013). The solution was stirred at a low speed for 24 h. Subsequently, the NPs were centrifuged at 8000 rpm for 40 min, and the pellets were stored at +4 °C for characterisation analysis. While wet pellets were used specifically for particle size and zeta potential analysis, lyophilised pellets were employed for other analyses.

Characterisation analysis of nanoparticles (NPs)

The particle morphology, size and structural composition of the NPs were assessed through FE-SEM, TEM, Zeta particle size, the polydispersity index (PDI), zeta potential analysis, as well as FT-IR, UV–Vis and TGA for characterisation purposes.

Surface morphologies of the NPs were examined using FE-SEM (Zeiss Sigma 300 VP, Carl Zeiss, Jena, Germany) scanning electron microscopy, operating at an acceleration voltage of 15 kV. Prior to SEM observation, the particle surfaces were coated with gold–palladium mixture to make the surface conductive.

The TEM analysis of the NPs was conducted by JEOL JEM-1400 Plus electron microscope instrument (JEOL Ltd., Tokyo, Japan) using an electron acceleration voltage of 80 kV. The samples were initially dispersed in water and subsequently dripped onto a carbon-coated copper grid. Following solvent evaporation, TEM analyses were performed.

Particle size distribution was evaluated using the Malvern Nano ZS 90 Zetasizer (Malvern Panalytical Ltd, UK) analyser at İzmir Katip Çelebi University Central Research Laboratories Application and Research Center (İzmir, Turkey). Particle size was measured by dynamic light scattering in the range of 1–8000 nm. Additionally, the PDI and zeta potential of the NPs were determined. Wet NP samples, collected after centrifugation, were dispersed in 5 mL of deionised water for 2 min prior to their introduction into the instrument. Up to 100 readings were selected for the analysis of each sample using the instrument's automatic mode. As the measurements were consistent during the analysis, the instrument performed 20 readings for each sample. Each sample was analysed as 20 readings and was averaged by repeating the analysis three times.

The infrared spectra of chitosan reference standard, developed Blank NP1, and TFNP were recorded using an FT-IR (FT-IR Spectrum One, Perkin Elmer, USA) spectrometer equipped with a universal attenuated total reflection (ATR) sampling accessory (4000–450 cm^{-1}) to examine the functional groups on the chemical structures. About 3.0 mg of samples were

used for the analysis. FT-IR spectrum with a resolution of 4 cm^{-1} was recorded by averaging four scans.

The UV–Vis absorption spectra of the chitosan reference standard and NPs covering a wavelength range from 240 nm to 800 nm were recorded in 1.5% (v/v) acetic acid using an Analytikjena Specord 210 Plus spectrophotometer (UK) at ambient temperature. The measurements were performed employing a quartz spectrophotometer cell with a path length of 1.0 cm.

The thermal properties of Blank NP1 and TFNP were investigated using a Perkin Elmer Diamond Thermal Analyser TGA-DTG-DTA (Shelton, Connecticut, USA) under a nitrogen flow with an adjusted flow rate of 200 mL min^{-1}. The heating rate employed was 10 °C per minute. Prior to the analysis, the samples were weighed (10 mg, dry weight) and placed in ceramic containers.

In vitro antioxidant activity analysis

Determination of antioxidant activity by 2,2-diphenyl-1-picrylhydrazyl (DPPH) method

Based on the method proposed by Brand-Williams *et al.* (1995), the antioxidant activity of the prepared extracts was evaluated using the DPPH radical scavenging method (Brand-Williams *et al.*, 1995). Minor modifications were made in this evaluation. A stock solution of Trolox was prepared by weighing 10.3 mg of 6-hydroxy-2,5,7,8-tetramethylchroman-2-carboxylic acid (Trolox) compound with 97% purity. The obtained Trolox was dissolved in 10 mL of methanol to prepare a 1000 μg mL^{-1} primary stock solution. Calibration standard solutions of Trolox were prepared at different concentrations (5 μg mL^{-1} to 100 μg mL^{-1}) by diluting the primary stock standard solution.

To prepare a 100 mL 10^{-4} M DPPH solution, 4.1 mg of DPPH with 97% purity was weighed and dissolved in methanol. For calibration, 100 μL aliquots of different concentrations of Trolox calibration standard solutions were pipetted, and 900 μL of 10^{-4} M DPPH solution was added. For the control, 100 μL aliquots of ethanol solution and all obtained samples in the study were each taken, and 900 μL of 10^{-4} M DPPH solution was added. The mixture was vortexed and then kept in the dark at room temperature for 30 min. Subsequently, absorbance values were measured at 517 nm using a JASCO V-650 spectrophotometer (JASCO, Japan). DPPH % radical scavenging rates were calculated using the formula provided in eq. 1.

$$\%\ \text{Radical Scavenging Activity} = [(A_{\text{control}} - A_{\text{extract or standard}})/A_{\text{control}}] \times 100 \quad (1)$$

A calibration curve was obtained based on the DPPH % radical scavenging-concentration relationship. Using the calibration curve, the total antioxidant capacity values of the samples were determined in mg Trolox equivalent (TE)/g extract. The analyses were performed in triplicate (Dursun *et al.*, 2024).

Determination of antioxidant activity using 2,2′-azino-bis (3-ethylbenzothiazoline-6-sulfonic acid) (ABTS)

The ABTS stock solution was prepared as described by Re *et al.* (1999) and allowed to stand in the dark at room temperature for 12–16 h (Re *et al.*, 1999). Calibration standards ranging from 5 μg mL^{-1} to 100 μg mL^{-1} were prepared in methanol solvent. Each standard was dispensed into capped test tubes at a volume of 2 mL, followed by the addition of 100 μL of ABTS working solution and 900 μL of ABTS assay solution for calibration. Additionally, all samples obtained in the study were added to test tubes at a volume of 100 μL, followed by the addition of 900 μL of ABTS assay solution. After 6 min, absorbances were determined at 734 nm. The ABTS % radical scavenging activity was calculated using the formula in eq. 1. Total antioxidant capacity values were determined in mg TE/g extract based on the calibration curve obtained from the ABTS % radical scavenging-concentration type. Analyses were performed in triplicate (Dursun *et al.*, 2024).

Statistical analysis

Analyses were performed in triplicate and these results are reported as mean and standard deviation (SD). The significance of differences between samples for zeta and antioxidant activity analysis results were determined by one-way analysis of variance (ANOVA) and the post hoc Tukey HSD test using IBM SPSS Statistics 27 at 0.05 significance level.

Results and discussion

Taxonomic description

Basidiomycota R.T. Moore, Agaricales Underw. Tricholomataceae R. Heim

Tricholoma fracticum (Britzelm.) Kreisel (Fig. 1).

Pileus; 30–100 mm, convex, expanding to nearly flat, sometimes the disc collapses inwards and the edge lifts in age, often wavy, becoming decurved, reddish brown, dark red-brown to orangish brown, faintly to not striate. Odour; mild or faintly of cucumbers. Taste; bitter, farinaceous. Stipe; 20–100 × 10–25 mm, more or less equal, or tapering to the base, surface cream-buff at the apex, annular zone membranous when young, pruinose to slightly fibrillose-striate, whitish near the apex, sometimes discolouring a little brownish; orangish brown below. Basidia; 34–42.5 × 6.8–8.1 μm, clavate, without basal clamp. Spores; 4.6–7.5 × 3.2–5.6 μm, smooth, subglobose to globose, elliptical, non-amyloid.

Figure 1 *Tricholoma fracticum* (a) Basidiocarps, (b) Basidia, (c) Basidiospores. Scale bar: 10 μm. Photo and microcharacters drawing by İsmail Acar.

The characterisation analysis results of nanoparticles (NPs)

Particle size and morphology of nanoparticles (NPs)

This study synthesised NPs using the methods outlined by Gokce (2008), Dhamodharan & Mirunalini (2013) and Canbolat *et al.* (2024) (Gokce, 2008; Dhamodharan & Mirunalini, 2013; Canbolat *et al.*, 2024). The preparation of Blank NPs relied on the ionic gelation method, involving the interaction between positively charged chitosan and negatively charged STPP, conducted at room temperature. Initially, the influence of the mass ratio of chitosan/STPP (w/w) on the formation and size of Blank NPs was determined using two different proportional methods. Zhang *et al.* (2004) suggested that the smallest NP size could be obtained with a chitosan/STPP (w/w) ratio of 5 (Zhang *et al.*, 2004). Hence, in this study, Blank NPs were synthesised at two different mass ratios (2-fold and 5-fold). Figure 2 depicts the ZETA particle size, PDI and ZETA potential value of Blank NP1 (Fig. 2a) and Blank NP2 (Fig. 2b) developed with two different mass ratios.

Upon examination of Table 1, it is observed that in Blank NP1 with a chitosan/STPP (w/w) ratio of 2, the mean particle size, PDI and zeta potential values are 265.5 ± 15.8 nm, 0.4 and 38.7 ± 4.0 mV, respectively (Fig. 2a). In comparison to the particle size, PDI and zeta potential values of Blank NP2 (chitosan/STPP ratio of 5) (Fig. 2b), it can be seen that under the same method conditions, Blank NP1 achieves a smaller particle size ($P < 0.05$), lower PDI value and higher zeta potential value than Blank NP2 ($P < 0.05$). According to the results of the zeta analysis, the shape of the chromatograms, zeta potential and low PDI values of Blank NP1 indicate stable and homogenous distribution of the developed Blank NP1 within the solvent.

Analysis of the FE-SEM and TEM results of the Blank NPs reveals a notable disparity between the two formulations. Sponge-like voids are observed in FE-SEM images of NPs (Fig. 3a,b). However, in TEM images, NPs appear spherical (Fig. 3c,d). Specifically, in the images of Blank NP1, the delineation of spherical particle shapes appears more pronounced compared to Blank NP2 (Fig. 3c,d). The Blank NP1, which closely matched the criteria recommended in the literature regarding shape and zeta values, was found to have different proportional levels from the study by Zhang *et al.* (2004). The chitosan NPs with less aggregation and greater stability were achieved when the chitosan/STPP ratio was 2-fold. Therefore, TFNPs were synthesised using the proportional method of Blank NP1.

Upon examination of the FE-SEM (Fig. 4a), TEM (Fig. 4b) images and ZETA values of TFNPs (Fig. 4c), it was found that the particle size increased to 333.2 ± 16.3 nm, and the zeta potential value was close to that of Blank NP1 (Table 1). Loading of mushroom extract led to an increase in particle size and closer proximity of particles observed in TEM images (Fig. 4b).

The biochemical impact of scaffolds played a crucial role in their practicality, demanding close attention to particle surface characteristics and particle size distribution (Jafarimanesh *et al.*, 2023). Zeta potential measurements were employed to assess the stability of the synthesised NPs, with higher magnitude potentials indicating increased electrostatic repulsion and, consequently, heightened stability. Generally, particles with zeta potentials falling within the 0–5 mV range tend to

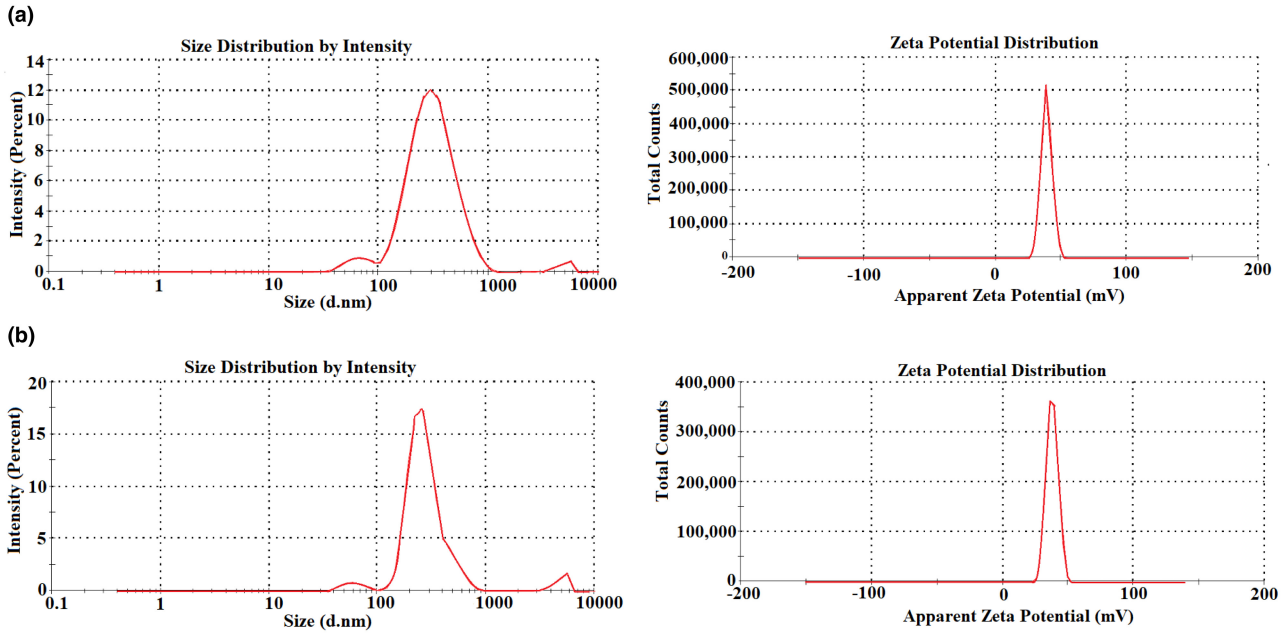

Figure 2 Zeta particle size and zeta potential analysis results of Blank NPs. (a) Blank NP1 (b) Blank NP2.

Table 1 Zeta analysis results of nanoparticles

Sample	Chitosan/STPP (w/w)	Particle Size (nm)	PDI	Potential (mV)
Blank NP1	2	265.5 ± 15.8a	0.4	38.7 ± 4.0a
Blank NP2	5	311.1 ± 14.4a	0.5	37.6 ± 4.4b
TFNP	2	333.2 ± 16.3a	0.4	37.0 ± 4.1b

Particle size and potential means of samples followed by different letters in a column are significantly different ($P < 0.05$).
Blank NP1, Blank chitosan nanoparticle (Chitosan/STPP ratio of 2-fold); Blank NP2, Blank chitosan nanoparticle (Chitosan/STPP ratio of 5-fold); PDI, polydispersity index; TFNP, *Tricholoma fracticum* Extract-Loaded Chitosan Nanoparticles.

aggregate or cluster, those within the 5–20 mV range exhibit stability, and those surpassing 20 mV are considered highly stable (Ates, 2018). Zeta potential measurement also confirms NP surface load performance as positive, negative or neutral (Acay *et al.*, 2020). Fig. 4c illustrates the zeta potential and particle size distribution of TFNPs measured via ZETA analysis. The intensity profile of particle size distribution, PDI and zeta potential values of TFNPs are depicted in Fig. 4c. The particle size of the obtained particles was approximately 333.2 nm. Negatively charged groups contribute to a decrease in zeta potential, while positively charged groups lead to an increase in zeta potential value (Acay *et al.*, 2020). As illustrated in Fig. 4c, the zeta potential value exhibited a notably positive value (37.0 mV). This positive value in the zeta potential may be attributed to positively charged functional groups within the TFNPs. In our study, all synthesised NPs had high zeta potential and stability. Polydispersed systems tend to aggregate more than monodisperse systems, with PDI as an aggregation indicator in particles. A high PDI value indicates greater polydispersity in nanosystems, while a low PDI value represents a more uniform, monodisperse system (Acay *et al.*, 2020). The proximity of the PDI values of all developed NPs to zero in our study suggests a homogeneous NP distribution, indicating similar sizes for each NP with narrow distributions. Furthermore, the sharpness of the zeta potential peak in Fig. 4c provides insights into the homogeneity of the structure (Canbolat *et al.*, 2024). In the study conducted by Acay *et al.* (2020), *Pleurotus eryngii* extract-loaded chitosan NPs were synthesised using the ionic gelation method. The particle size, zeta potential and PDI value of the developed mushroom-loaded chitosan NPs were reported as 330.1 nm, 8.1 mV and 0.6, respectively, in the study (Acay *et al.*, 2020). In our study, while the particle size of TFNPs was similar to those reported by Acay et al., the zeta potential values of our NPs were higher, indicating enhanced stability. Additionally, the low PDI values of the synthesised NPs in our study are important in terms of the applicability and usability of the method. When examining the zeta analysis results, the chromatograms' sharpness and the

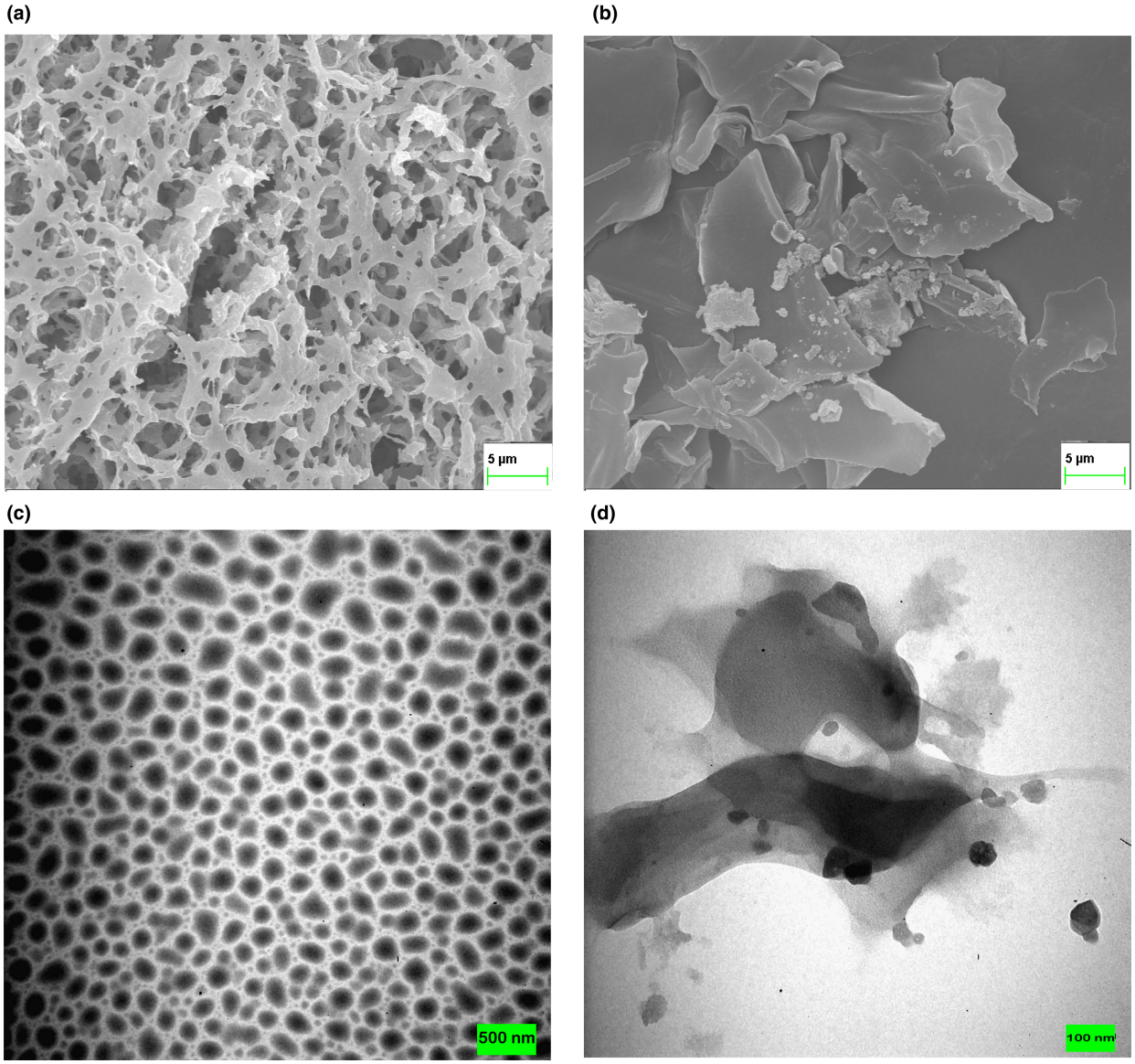

Figure 3 Field emission scanning electron microscopy (FE-SEM) and Transmission electron microscopy (TEM) analysis results of Blank NPs. (a) FE-SEM results of Blank NP1, (b) FE-SEM results of Blank NP2, (c) TEM results of Blank NP1, (d) TEM results of Blank NP2.

potential values indicate a stable and homogeneous distribution of the developed NPs within the solution. All obtained results suggest that drugs were homogeneously loaded into NPs, with uniform distribution, potentially enhancing drug transport efficiency and contributing to the improved bioavailability of bioactive molecules.

Structural analyses of nanoparticles (NPs)

Fourier-transform infrared spectra of chitosan, Blank NP1 and TFNP are given in Fig. 5a. According to the FT-IR spectrum of the chitosan stretching peak at 3281 cm^{-1} was attributed to a band of O–H can be seen overlapping with N–H peak. The spectral bands of chitosan at 2925 cm^{-1} and 2852 cm^{-1} represent aliphatic C–H stretching vibrations. Three types of amide groups of chitosan, which were seen at 1642 cm^{-1}, 1544 cm^{-1} and 1378 cm^{-1}, correspond to amide C = O stretching (amide I), N–H bending (amide II) and C–N stretching (amide III), respectively. Additionally, the peak at 1070 cm^{-1} represents C–O stretching vibration (Rahman *et al.*, 2019).

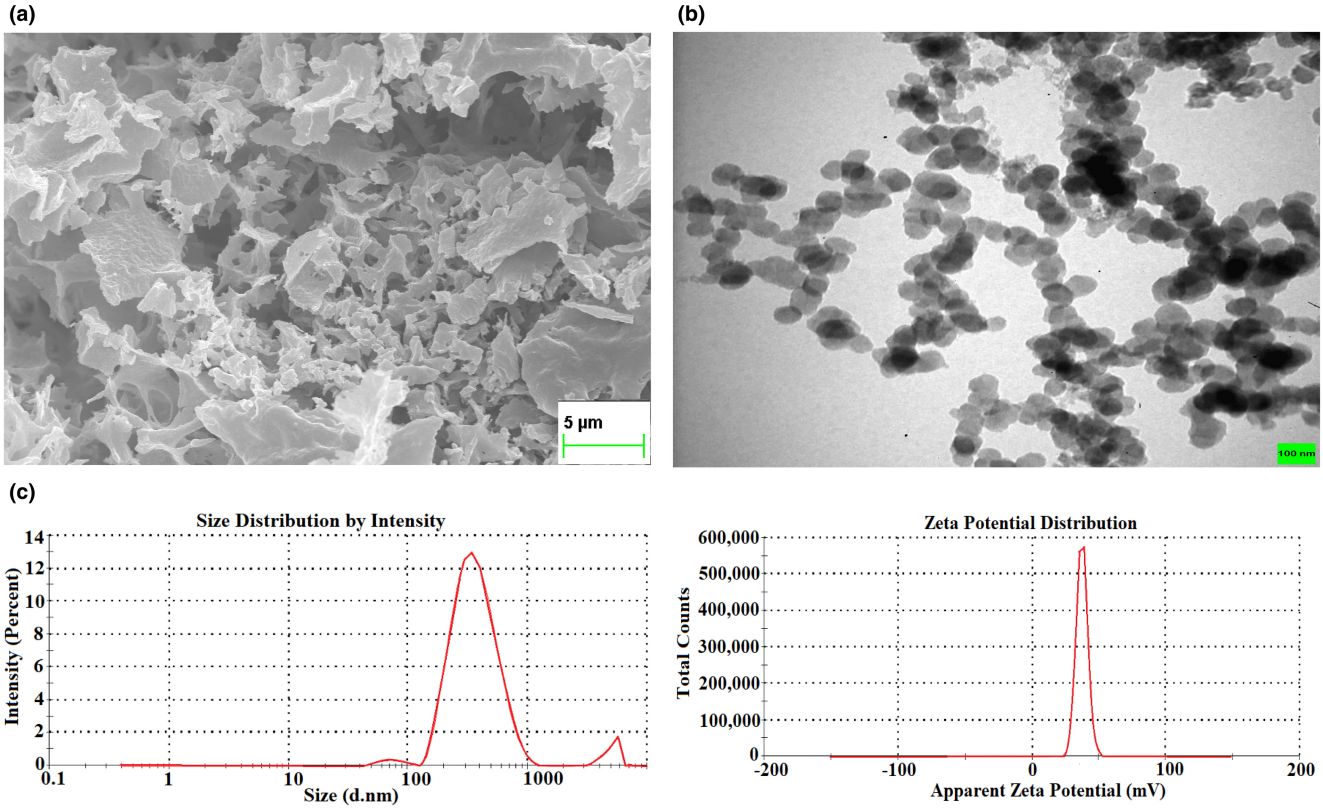

Figure 4 Zeta, field emission scanning electron microscopy (FE-SEM) and transmission electron microscopy (TEM) results of *T. fracticum* Extract-Loaded Chitosan Nanoparticles (TFNPs). (a) SEM, (b) TEM, (c) Zeta particle size and potential.

The FT-IR spectrum of Blank NP1 consists of a broad absorption peak at 3323 cm^{-1} due to OH groups. The broad OH peak is due to the intermolecular hydrogen bonds formed between the polyphenolic compounds and β-glucan or intramolecular hydrogen bonds within these molecules. Since polysaccharides are one of the major components of fungi, the peaks at 971 cm^{-1} and 837 cm^{-1} indicate the presence of β-glucan in the structure. The peaks of the polyphenolic compounds' C–O–C glycosidic linkages of β-glucan and primary alcohols groups (C–O–H) were seen at 1081 and 1056 cm^{-1}, respectively. Additionally, the CH_2 bending vibrations peaks of β-glucan and polyphenolic compounds were observed at 1460 and 1409 cm^{1}. Strong CH aliphatic stretching peaks (2922 and 2855 cm^{-1}) and C–H deformation peaks (in the range of 913–725 cm^{-1}) of β-glucan were observed (Koc *et al.*, 2020).

According to the FT-IR spectrum of TFNP, the C–H aliphatic stretching vibration peaks are observed at 2925 and 2849 cm^{-1}. The amide II band of chitosan (1541 cm^{-1}) was observed overlapping with the C=C stretching peak of polyphenolic compounds. The peaks of C–O–C glycosidic linkages and C–O–H groups were broadened of the β-glucan and polyphenolic compounds (Koc *et al.*, 2020).

Figure 5b shows the UV–Vis spectra of chitosan, Blank NP1 and TFNP in the 240–800 nm wavelength range. The recorded UV–Vis spectrum of pure chitosan revealed two maximum absorption peaks (λ_{max}) at 255 nm and 286 nm, corresponding to the π→π* transition of chitosan (Thamilarasan *et al.*, 2018). UV–visible spectrum scanning of the synthesised blank NP1 revealed two prominent peaks (λ_{max}) at 328 nm and 392 nm, associated with $n\rightarrow\pi^*$ transitions of –P=O– and –OH functional groups present in STPP, an essential component used in the formation of chitosan NPs. Due to the inclusion of phenolic and flavonoid compounds within TFNP, distinct peaks were detected at 272, 284, 296 and 312 nm, indicative of the π→π* and $n\rightarrow\pi^*$ transitions occurring within the system.

The weight loss behaviour and maximum weight loss temperature of Blank NP1 and TFNP were determined over a temperature range from 20 °C to 1000 °C, as depicted in Fig. 6. Up to a temperature of 150 °C, both blank NP1 and TFNP displayed weight losses of

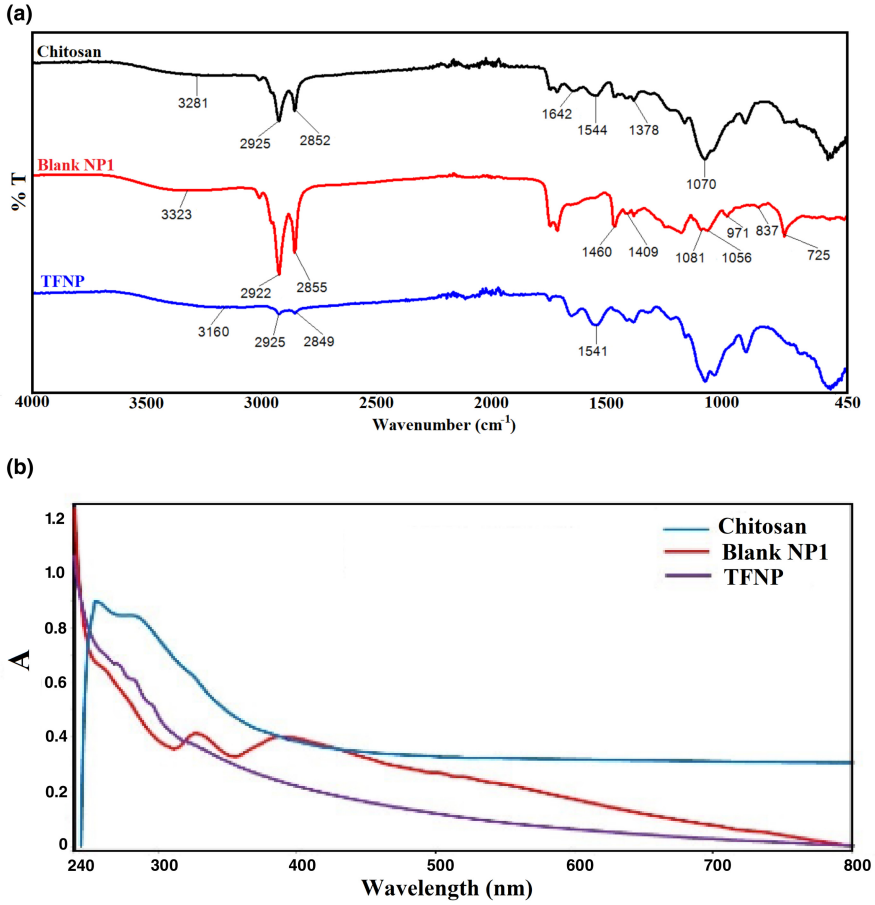

Figure 5 Fourier-transform infrared (FT-IR) and UV–Vis absorption spectra of samples. (a) FT-IR spectra, (b) UV–Vis absorption spectra. Blank NP1; Blank chitosan nanoparticle (Chitosan/STPP ratio of 2-fold), TFNP; Tricholoma fracticum Extract-Loaded Chitosan Nanoparticle.

13.60% and 12.70%, respectively, which can be ascribed to the evaporation of water and solvents, such as acetic acid and water, inherent in the samples. As observed in the thermogravimetric curves (Fig. 6a), Blank NP1 and TFNP degradation initiated at (T_{on}) 218 °C and 223 °C, respectively. Blank NP1 underwent a two-step degradation process. The decomposition temperature at maximum weight loss rate (T_{max}) values for Blank NP1 were 244 °C and 957 °C (Fig. 6b), signifying the degradation of chitosan resulting from the decomposition of amide groups and the main C–O–C chain, respectively (Kumar *et al.*, 2023). The weight loss observed in the temperature range from 150 °C to 464 °C was found to be 41.68%. A subsequent weight loss from 464 °C to 1000 °C was calculated to be 33.08%. Regarding the TFNPs, the T_{max} values were 246 °C, 357 °C and 900 °C, associated with a three-step degradation (Fig. 6b). The first degradation step took place between 150 °C and 312 °C with a mass loss of 32.08% of TFNP. The second thermal degradation, occurring within the temperature range of 312 °C to 464 °C with a maximum peak at 357 °C, was observed for chitosan-*T. fracticum* extract, attributable to the degradation of the *T. fracticum* extract component (Koc *et al.*, 2020). As the temperature increased to 1000 °C, the weight loss of 22.77% was due to the degradation of chitosan and the main chain within TFNP.

At 1000 °C, Blank NP1 exhibited a residual amount of 25.24%. The remaining residue in TFNP was primarily attributed to the gradual carbonisation of phenolic and flavonoid content within the nanoparticles, resulting in an increased residual amount of 27.65%. Notably, the presence of phenolic and flavonoid content in TFNP suggested a significant interaction between phenolic and flavonoid content and the chitosan of NP1. This interaction resulted in enhanced structural and chemical stability of TFNP.

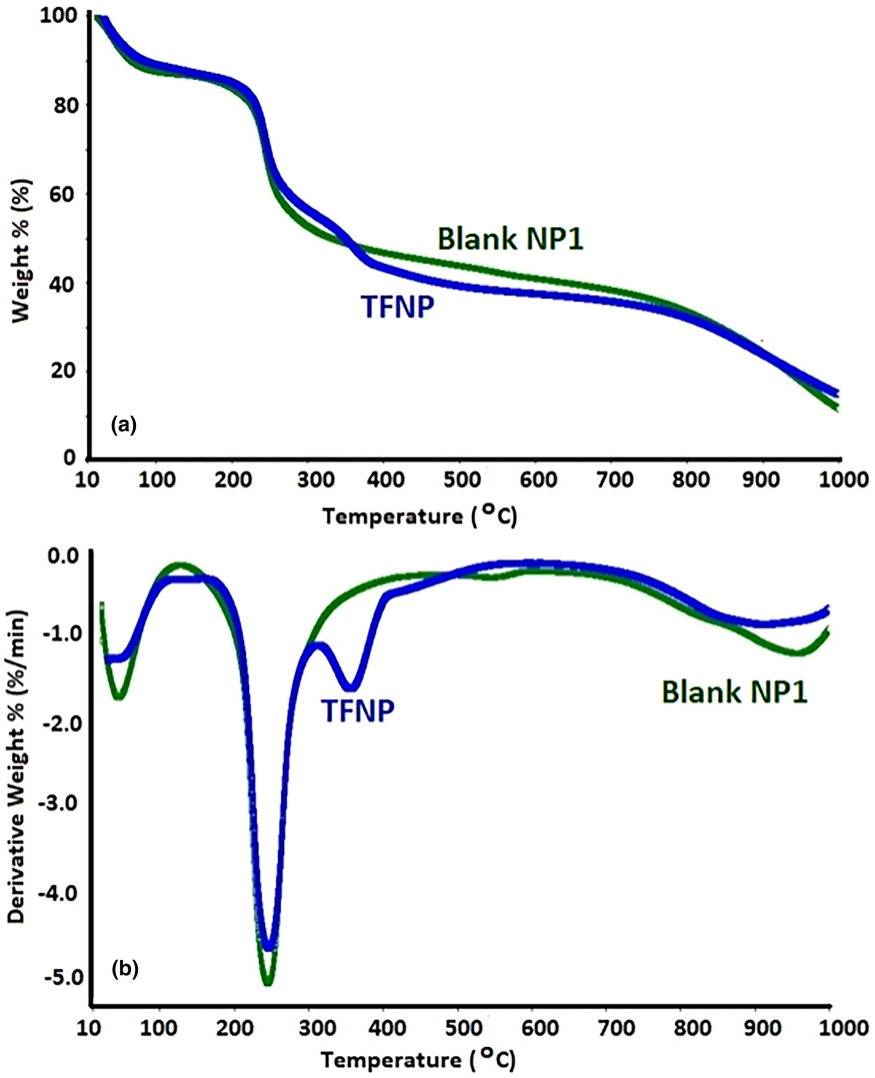

Figure 6 Thermogravimetric analysis (TGA) results of samples. (a) Thermogravimetric (TG) curve, (b) Derivative of the thermogravimetric (DTG) curve. NP1, Blank chitosan nanoparticle (Chitosan/STPP ratio of 2-fold); TFNP, *Tricholoma fracticum* Extract-Loaded Chitosan Nanoparticle.

Fenolic and flavonoid content in *Tricholoma fracticum* extract

Prior to evaluating the antioxidant activity of the samples, the phenolic and flavonoid contents of the *T. fracticum* extract, obtained via ethanol extraction (0.7% extraction yield (w/w)), were determined through spectroscopic and chromatographic analysis (Table 2). Phenolic content was determined relative to GA standards, while flavonoid level was quantified relative to QE equivalents.

Table 2 reveals that the amount of phenolic compounds in the *T. fracticum* ethanol extract was 7.1 ± 0.3 mg GAE/g extract using the Folin–Ciocalteu analysis method. The flavonoid content in the *T. fracticum* ethanol extract was 5.5 ± 0.6 mg QUE/g extract. Phenolic compounds are directly involved in antioxidative actions, and their content is closely associated with antioxidant activity (Tel *et al*., 2012). The antioxidant activity of phenolic generally correlates with their chemical structures, with increased activity observed as the number and position of hydroxyl groups within the molecules increase (Dhamodharan & Mirunalini, 2013). Therefore, total phenolic content plays a crucial role in the antioxidant activity of mushroom extracts (Tel *et al*., 2012). In our study, the ethanol-extracted mushroom exhibited a yield of 0.68%. The phenolic and flavonoid contents in the extract were determined to be 7.1 ± 0.3 mg and

Table 2 Results of phenolic and flavonoid compounds in *T. fracticum* ethanol extract and *in vitro* antioxidant activity analysis of the samples

Sample	Extraction yield (% w/w)	Amount of fenolic and flavonoid		Antioxidant activity analysis	
		Fenolic (mg GAE/g extract)	Flavonoid (mg Que/g extract)	DPPH (mgTE/g extract)	ABTS (mgTE/g extract)
T. fracticum	0.7	7.1 ± 0.3	5.5 ± 0.6	1.2 ± 0.1a	4.2 ± 0.1a
TFNP				2.0 ± 0.2c	8.1 ± 0.1c
Chitosan				0.4 ± 0.1b	2.3 ± 0.2b
Blank NP1				0.3 ± 0.1b	2.3 ± 0.2b

Amount of phenolic compound in *T. fracticum* ethanol extract using Exactive Plus Orbitrap LC-MS

Sample	Molecule	Retention time (RT; minute)	Quantitative ion (m/z)	Calibration range (ng mL^{-1})	Concentration (ng mL^{-1})
T. fracticum	Benzoic acid	10.84	121.02950	10–1000	5.3 ± 0.3
	4-hydroxybenzoic acid	7.86	137.02442		11.6 ± 0.5
	Syringic acid	8.92	197.04555		3.9 ± 0.2
	Trans cinnamic acid	12.31	147.04515		12.6 ± 1.3
	Quinic acid	0.94	191.05611		12.5 ± 0.3
	Galangin	14.59	269.04555		2.4 ± 0.2
	Quercetin	12.22	301.03538		2.5 ± 0.0

DPPH and ABTS activity means of samples followed by different letters in a column are significantly different ($P < 0.05$). Values are the mean of triplicate measurements.
Blank NP1, Blank chitosan nanoparticle (Chitosan/STPP ratio of 2-fold); TFNP, *Tricholoma fracticum* Extract-Loaded Chitosan Nanoparticle.

5.5 ± 0.6 mg, respectively. Dhamodharan & Mirunalini (2013) reported a phenolic content of 8.2 ± 1 mg of GA equivalents per gram of sample in ethanol-extracted mushrooms (Dhamodharan & Mirunalini, 2013), consistent with our findings. However, variations in phenolic content can arise from the use of different extraction solvents (Tel *et al.*, 2012; Sadi *et al.*, 2015). Since our study utilised a single solvent type, the influence of alternative solvents on phenolic content was not investigated. Tel *et al.* (2012) analysed the phenolic content and bioactivity of *Tricholoma* species extracted using different solvents (Tel *et al.*, 2012). The ethyl acetate extract of *T. terreum* exhibited the highest phenolic content among the tested extracts, while the methanol extract of *T. fracticum* exhibited the highest flavonoid content. In our study, the phenolic and flavonoid content in *T. fracticum* extracted with ethanol was lower than the values reported by Tel *et al.* (2012), suggesting potential solvent-related variations influencing our findings.

Chromatographic analysis of the ethanol extract of *T. fracticum*, employing calibration standards comprising 77 phenolic compound standards, revealed the presence of seven phenolic compounds within the mushroom content (Figure S1). Specifically, 11.6 ± 0.5 ng mL^{-1} of 4-hydroxybenzoic acid, 12.6 ± 1.3 ng mL^{-1} of trans cinnamic acid and 12.5 ± 0.3 ng mL^{-1} of quinic acid were detected. However, benzoic acid, syringic acid, galangin, Que were found to be below the lowest calibration standard concentration (Table 2).

These seven molecules have been recognised in the literature not only for their antioxidant activities but also for their various pharmacological properties as bioactive substances found in mushroom extracts (Ribeiro *et al.*, 2006; Li *et al.*, 2014; Tanaka *et al.*, 2019; Cayan *et al.*, 2020; Miranda *et al.*, 2021; Li & Bao, 2022). Cayan *et al.* (2020) identified trans cinnamic acid in twenty-six mushroom species in their study (Cayan *et al.*, 2020). Similarly, our study detected trans cinnamic acid as one of the main bioactive molecules in the ethanolic extract of *T. fracticum*. Ribeiro *et al.* (2006) reported the presence of quinic acid in the analysed mushroom species in dried Portuguese wild edible mushrooms (Ribeiro *et al.*, 2006). Analyses conducted on *Tricholoma equestre* mushrooms reported 4-hydroxybenzoic acid as the most abundant phenolic compound (Miranda *et al.*, 2021). Similarly, in our study, 4-hydroxybenzoic acid stood out as one of prominent molecules in the extract of *T. Fracticum*, a species belonging to the *Tricholama* species. Our findings indicate that the bioactive compound types extracted from *T. fracticum* in our study align with those identified in various other mushroom species documented in the literature (Li & Bao, 2022).

In vitro antioxidant activity analysis results

Upon examining Table 2, the levels of phenolic and flavonoid compounds in the *T. fracticum* ethanol extract are presented regarding mg TE. A higher TE

signifies elevated antioxidant activity. In our study, statistically significant differences were observed within each sample group regarding the antioxidant activities of *T. fracticum* and TFNP in DPPH analysis ($P < 0.05$) (Table 2). However, when comparing the antioxidant activity of chitosan and Blank NP1, no significant difference was found between the two ($P > 0.05$). In contrast, the antioxidant activity of these samples was statistically significantly lower compared to *T. fracticum* and TFNP ($P < 0.05$). Similar results and statistical significance were also detected in the ABTS analyses of the samples ($P < 0.05$). In this context, the antioxidant activities of the samples, as determined by DPPH analysis, follow a descending order from highest to lowest: TFNP, *T. fracticum* extract, chitosan reference, Blank NP1. The ABTS antioxidant activity analysis results also confirm the DPPH analysis results. Among our findings, it was observed that encapsulated *T. fracticum* exhibited higher antioxidant activity compared to its free form. Several factors may contribute to this observation. Bagheri *et al.* (2021) reported chitosan NPs loaded with vegetable oil demonstrated higher antioxidant activity free vegetable oils (Bagheri *et al.*, 2021). Similarly, Soleymanfallah *et al.* (2022) reported that the antioxidant activity of chitosan NPs loaded with plant extract was higher than that of free plant extract (Soleymanfallah *et al.*, 2022). Alqahtani *et al.* (2021) reported that, depending on the concentration, plant extract-loaded chitosan nanoparticles exhibited equivalent to or slightly higher antioxidant activity than free plant extracts (Alqahtani *et al.*, 2021). In the light of the findings in the literature and in our study, several factors contribute to this phenomenon: (i) Encapsulation processes protect plant extracts from oxygen and temperature-induced degradation, thereby reducing the evaporation rate of volatile components and potentially preserving or even enhancing antioxidant activity compared to free forms. (ii) Encapsulation may protect the hydroxyl groups of phenolic compounds within the extract, thereby maintaining their free radical scavenging activity. Further comprehensive research is warranted to fully elucidate these mechanisms.

Researchers have determined that the bioactive compound content in mushrooms is the source of their antioxidant properties. Various mushrooms contain potent antioxidants such as phenolics, flavonoids, glycosides, polysaccharides, tocopherols, ergothioneine and carotenoids, which are extracted from their fruiting bodies, mycelium and aqueous solutions (Chun *et al.*, 2021). *T. fracticum* belongs to the group of ectomycorrhizal fungi, which form symbiotic relationships with higher plants. Although *T. fracticum* is known to be an edible mushroom with potential medicinal uses, it is described as having a slightly bitter and tough taste (Tel *et al.*, 2012; Qonitah *et al.*, 2023). To overcome these limitations, it is important to develop different formulations to facilitate the use of *T. fracticum* and similar mushroom species and to benefit from their pharmacological properties. Additionally, it is desired to preserve the bioactivities of bioactive compounds in different formulations. Therefore, the antioxidant activities of mushroom extract-loaded NPs developed using nanotechnological methods are expected to continue following encapsulation. Antioxidant activity tests are performed using various methods documented in the literature. Due to the chemical complexity of the extracts, which consist of a combination of numerous compounds exhibiting varied functional groups, polarity and chemical behaviour, outcomes can diverge significantly depending on the test used. Therefore, commonly used antioxidant potential evaluation methods in the literature, such as DPPH radical scavenging and ABTS cation radical scavenging assays (Acar *et al.*, 2021; Kartal *et al.*, 2022; Canbolat & Ates, 2023; Canbolat *et al.*, 2024), were utilised in our study. The DPPH results of the analysed samples varied between 0.3 and 2 mg TE/g extract, while the ABTS test results ranged from 2.3 to 8.1 mg TE/g extract in our study (Table 2). Given the paucity of research on the antioxidant capacity of *T. fracticum*, comparisons are drawn with studies analysing the antioxidant activity of other mushrooms within the *Tricholoma* family and/or different mushroom species.

In the study by Bal (2021), the antioxidant potential of *Tricholoma imbricatum* was analysed. The study found that the Total Antioxidant Status (TAS) value of *T. imbricatum* was determined to be 3.5 ± 0.1, with a Total Oxidant Status (TOS) value of 15.3 ± 0.1 (Bal, 2021). Sadi *et al.* (2015) found that *T. fracticum* acetone extract exhibited antioxidant activity using the DPPH method (Sadi *et al.*, 2015). Baptista *et al.* (2023) conducted a bioactivity analysis of *Lentinula edodes*' spent mushroom substrate using different extraction methods. The DPPH test results ranged from 0.2 to 1.5 mmol Trolox/g extract, while the ABTS test results ranged from 0.4 to 0.9 mmol Trolox (Baptista *et al.*, 2023). In research by Dhamodharan & Mirunalini (2013), chitosan nanoparticles loaded with *Agaricus bisporus* extract were studied for bioactivity, demonstrating preserved antioxidant activity post-encapsulation (Dhamodharan & Mirunalini, 2013).

The DPPH assay results ranged from 0.2 to 1.5 mmol Trolox/g extract, while the ABTS assay results ranged from 0.4 to 0.9 mmol trolox (Baptista *et al.*, 2023). In research by Dhamodharan & Mirunalini (2013), chitosan nanoparticles loaded with Agaricus bisporus extract were studied for bioactivity, demonstrating preserved antioxidant activity post-encapsulation (Dhamodharan & Mirunalini, 2013).

In our study, the antioxidant activity of *T. fracticum* extract determined by both DPPH and ABTS analyses remained preserved after encapsulation and demonstrated a partial increase (Table 2). This increase is attributed to

the antioxidant effect of chitosan. Many studies in the literature have reported the antioxidant activity of chitosan (Savin *et al*., 2020; Shehabeldine *et al*., 2022).

Our analysis revealed that the ethanol extract of *T. fracticum*, which contains bioactive molecules such as trans cinnamic acid, quinic acid and 4-hydroxybenzoic acid alongside antioxidant properties, could be successfully loaded onto chitosan/STPP at a two-fold ratio using the ionic gelation method. Notably, the antioxidant activity of the *T. fracticum* extract was both partially enhanced and preserved. This finding indicates that the feasibility of loading *T. fracticum* and similar mushroom extracts onto chitosan, demonstrating the potential to preserve their bioactive properties when encapsulated.

Conclusion

Our results showed that the ethanol extract of *T. fracticum* could be easily and successfully loaded into chitosan using ionic gelation method. Importantly, it was observed that the antioxidant activity of *T. fracticum* extract persisted in the encapsulation state. These results suggested that *T. fracticum* may have potential for applications in therapeutic and functional food. Furthermore, the synthesis method developed in this study may offer potential for creating new nanoparticles tailored for various fungus species. The data from our study is anticipated to serve as a guiding source for advancing nanotechnological applications in the food and health industry.

Acknowledgments

We would like to thank Prof. Dr. İsmet Kaya and Assoc. Dr. Feyza Kolcu for their scientific and laboratory support.

Author contributions

Fadime Canbolat: Conceptualization (equal); data curation (equal); formal analysis (equal); investigation (equal); methodology (equal); resources (equal); validation (equal); visualization (equal); writing – original draft (equal); writing – review and editing (equal). **İsmail Acar:** Conceptualization (equal); investigation (equal); resources (equal); visualization (equal); writing – original draft (equal); writing – review and editing (equal). **Ruhiye Nilay Tezel:** Conceptualization (equal); investigation (equal); validation (equal); visualization (equal); writing – original draft (equal); writing – review and editing (equal).

Funding

The authors declare that this study received no funding.

Conflict of interest

The authors declare that they have no known competing financial interests or personal relationships that could have appeared to influence the work reported in this paper.

Ethics approval

This paper does not require ethical approval.

Informed consent

Not applicable.

Peer review

The peer review history for this article is available at https://www.webofscience.com/api/gateway/wos/peer-review/10.1111/ijfs.17585.

Data availability statement

Data will be made available on request.

References

Acar, İ., Blando, F., Gul, B. *et al*. (2021). The phenolic profile and biological activities of the wild-edible mushrooms *Helvella leucopus* and *Morchella pulchella*. *Journal of Food Measurement and Characterization*, **15**, 555–566.

Acay, H., Yildirim, A., Erdem Güzel, E., Kaya, N. & Baran, M.F. (2020). Evaluation and characterization of *Pleurotus eryngii* extract-loaded chitosan nanoparticles as antimicrobial agents against some human pathogens. *Preparative Biochemistry & Biotechnology*, **50**, 897–906.

Acay, H., Yildirim, A., Guney, I.G. & Dervis, S. (2022). *Morchella esculenta*-based chitosan bionanocomposites: evaluation as an antifungal agent. *Journal of Food Processing and Preservation*, **46**, 1–10.

Agarwal, M., Agarwal, M.K., Shrivastav, N., Pandey, S., Das, R. & Gaur, P. (2018). Preparation of chitosan nanoparticles and their in-vitro characterization. *International Journal of Life-Sciences Scientific Research*, **4**, 1713–1720.

Akdeniz, F., Dursun, İ., Tepebaş, K., Ozbay, H., Kekeç, L. & Yıldız, S. (2021). Comparison of different extraction methods for total phenolic content and antioxidant activity of dried *Diospyros lotus* L fruits. *Turkish Journal of Analytical Chemistry*, **3**, 64–69.

Aljebory, A.M. & Alsalman, T.M. (2017). Chitosan nanoparticles. *Imperial Journal of Interdisciplinary Research*, **3**, 233–242.

Alkin, M., Söğüt, E. & Seydim, A.C. (2021). Determination of bioactive properties of different edible mushrooms from Turkey. *Journal of Food Measurement and Characterization*, **15**, 3608–3617.

Allı, H. & Şen, I. (2016). *Tricholoma* türlerinin yenilebilirliği üzerine notlar. *Turkish Journal of Agriculture-Food Science and Technology*, **4**, 178–181.

Alqahtani, M.S., Al-Yousef, H.M., Alqahtani, A.S. *et al*. (2021). Preparation, characterization, and in vitro-in silico biological activities of *Jatropha pelargoniifolia* extract loaded chitosan nanoparticles. *International Journal of Pharmaceutics*, **606**, 1–9.

Altıntas, Ö.E. (2023). Evaluation of nutritional composition, antioxidant activities and anti-cancer effect of edible and medicinal

mushroom *Hericium erinaceus*. *Journal of the Institute of Science and Technology*, **13**, 2622–2633.
Ates, M. (2018). Measuring and inspection techniques of nanoparticles. *Turkish Journal of Scientific Reviews*, **11**, 63–69.
Bagheri, R., Ariaii, P. & Motamedzadegan, A. (2021). Characterization, antioxidant and antibacterial activities of chitosan nanoparticles loaded with nettle essential oil. *Journal of Food Measurement and Characterization*, **15**, 1395–1402.
Bal, C. (2021). Antioxidant potential and element contents of wild mushroom *Tricholoma imbricatum*. *KSU Journal of Agriculture and Nature*, **24**, 196–199.
Baptista, F., Campos, J., Costa-Silva, V. *et al.* (2023). Nutraceutical potential of *Lentinula edodes*' spent mushroom substrate: a comprehensive study on phenolic composition, antioxidant activity, and antibacterial effects. *Journal of Fungi*, **9**, 1200.
Barros, L., Calhelha, R.C., Vaz, J.A., Ferreira, I.C., Baptista, P. & Estevinho, L.M. (2007). Antimicrobial activity and bioactive compounds of Portuguese wild edible mushrooms methanolic extracts. *European Food Research and Technology*, **225**, 151–156.
Bodnar, M., Hartmann, J.F. & Borbely, J. (2005). Preparation and characterization of chitosan-based nanoparticles. *Biomacromolecules*, **6**, 2521–2527.
Brand-Williams, W., Cuvelier, M.E. & Berset, C.L.W.T. (1995). Use of a free radical method to evaluate antioxidant activity. *LWT – Food Science and Technology*, **28**, 25–30.
Canbolat, F. & Ates, G.O. (2023). Evaluation of the bioactivities of turmeric spices of different origins. *Anatolian Journal of Botany*, **7**, 154–160.
Canbolat, F., Demir, N., Yayıntas, O.T. *et al.* (2024). Chitosan nanoparticles loaded with quercetin and valproic acid: a novel approach for enhancing antioxidant activity against oxidative stress in the SH-SY5Y human neuroblastoma cell line. *Biomedicine*, **12**, 287.
Cayan, F., Deveci, E., Tel-Çayan, G. & Duru, M.E. (2020). Identification and quantification of phenolic acid compounds of twenty-six mushrooms by HPLC–DAD. *Journal of Food Measurement and Characterization*, **14**, 1690–1698.
Chun, S., Gopal, J. & Muthu, M. (2021). Antioxidant activity of mushroom extracts/polysaccharides-their antiviral properties and plausible antiCOVID-19 properties. *Antioxidants*, **10**, 1899.
Dhamodharan, G. & Mirunalini, S. (2013). A detail study of phytochemical screening, antioxidant potential and acute toxicity of *Agaricus bisporus* extract and its chitosan loaded nanoparticles. *Journal of Pharmacy Research*, **6**, 818–822.
Dursun, I., Felek, I. & Cobanoglu, D.N. (2024). Analyzing the antioxidant activity and fatty acid composition of monofloral mullein (*Verbascum* sp.) pollen oil obtained via various extraction techniques. *Chemistry & Biodiversity*, **21**, e202400117.
Ercan, L. (2024). Bioactive components, antioxidant capacity, and antimicrobial activity of *Berberis crataegina* fruit. *Pharmacological Research-Natural Products*, **2**, 100020.
Gao, Y. & Wu, Y. (2022). Recent advances of chitosan-based nanoparticles for biomedical and biotechnological applications. *International Journal of Biological Macromolecules*, **203**, 379–388.
Gokce, Y. (2008). *Kitosan Nanoparçacıklarının Sentezi*. Pp. 1–92. Master's thesis, Ankara, Turkey: Ankara University Institute of Science and Technology, Chemical Engineering.
Jafarimanesh, M.A., Ai, J., Shojaei, S., Khonakdar, H.A., Darbemamieh, G. & Shirian, S. (2023). Sustained release of valproic acid loaded on chitosan nanoparticles within hybrid of alginate/chitosan hydrogel with/without stem cells in regeneration of spinal cord injury. *Progress in Biomaterials*, **12**, 75–86.
Jardim, K.V., Siqueira, J.L.N., Báo, S.N. & Parize, A.L. (2022). In vitro cytotoxic and antioxidant evaluation of quercetin loaded in ionic cross-linked chitosan nanoparticles. *Journal of Drug Delivery Science and Technology*, **74**, 103561.
Karimirad, R., Behnamian, M. & Dezhsetan, S. (2020). Bitter orange oil incorporated into chitosan nanoparticles: preparation, characterization and their potential application on antioxidant and antimicrobial characteristics of white button mushroom. *Food Hydrocolloids*, **100**, 105387.
Kartal, D.I., Şayak, O. & Acar, I. (2022). Investigation of antioxidant activities of *Agrocybe praecox* fungus. *The Journal of Fungus*, **13**, 37–43.
Koc, B., Akyuz, L., Cakmak, Y.S. *et al.* (2020). Production and characterization of chitosan-fungal extract films. *Food Bioscience*, **35**, 100545.
Kumar, K., Mehra, R., Guiné, R.P. *et al.* (2021). Edible mushrooms: a comprehensive review on bioactive compounds with health benefits and processing aspects. *Food*, **10**, 2996.
Kumar, H., Ahuja, A., Kadam, A.A. & Rastogi, V.K. (2023). Antioxidant film based on chitosan and tulsi essential oil for food packaging. *Food and Bioprocess Technology*, **16**, 342–355.
Li, Z. & Bao, H. (2022). Comparative analysis of metabolic compositions and trace elements of *Inonotus hispidus* mushroom grown on five different tree species. *ACS Omega*, **7**, 9343–9358.
Li, H., Lee, H.S., Kim, S.H., Moon, B. & Lee, C. (2014). Antioxidant and antiinflammatory activities of methanol extracts of *Tremella fuciformis* and its major phenolic acids. *Journal of Food Science*, **79**, 460–468.
Miranda, C.F., Pessoa, A., Batista, M. *et al.* (2021). Ros signals induced by mushrooms phenolic compounds produced from lignocellulosic biomass. *Waste and Biomass Valorization*, **12**, 3027–3033.
Morin-Crini, N., Lichtfouse, E., Torri, G. & Crini, G. (2019). Applications of chitosan in food, pharmaceuticals, medicine, cosmetics, agriculture, textiles, pulp and paper, biotechnology, and environmental chemistry. *Environmental Chemistry Letters*, **17**, 1667–1692.
Qonitah, T.A., Aryyanto, M.R.A., Suteja, H., Murti, A.P. & Noverita, N. (2023). Edible mushrooms in the surroundings of Bangbayang Village, Situraja, Sumedang, West Java. *Journal of Tropical Biodiversity*, **4**, 25–38.
Rahman, N.A., Abu Hanifah, S., Mobarak, N.N. *et al.* (2019). Synthesis and characterizations of o-nitrochitosan based biopolymer electrolyte for electrochemical devices. *PLoS One*, **14**, e0212066.
Re, R., Pellegrini, N., Proteggente, A., Pannala, A., Yang, M. & Rice-Evans, C. (1999). Antioxidant activity applying an improved ABTS radical cation decolorization assay. *Free Radical Biology and Medicine*, **26**, 1231–1237.
Ribeiro, B., Rangel, J., Valentão, P., Baptista, P., Seabra, R.M. & Andrade, P.B. (2006). Contents of carboxylic acids and two phenolics and antioxidant activity of dried Portuguese wild edible mushrooms. *Journal of Agricultural and Food Chemistry*, **54**, 8530–8537.
Sadi, G., Emsen, B., Kaya, A., Kocabaş, A., Çınar, S. & Kartal, D.I. (2015). Cytotoxicity of some edible mushrooms extracts over liver hepatocellular carcinoma cells in conjunction with their antioxidant and antibacterial properties. *Pharmacognosy Magazine*, **11**, 6–18.
Sánchez, C. (2010). Cultivation of *Pleurotus ostreatus* and other edible mushrooms. *Applied Microbiology and Biotechnology*, **85**, 1321–1337.
Sandeep, A., Sangameshwar, K., Mukesh, G., Chandrakant, R. & Avinash, D. (2013). A brief overview on chitosan applications. *Indo American Journal of Pharmaceutical Research*, **13**, 1564–1574.
Savin, S., Craciunescu, O., Oancea, A. *et al.* (2020). Antioxidant, cytotoxic and antimicrobial activity of chitosan preparations extracted from *Ganoderma lucidum* mushroom. *Chemistry & Biodiversity*, **17**, e2000175.
Shehabeldine, A.M., Salem, S.S., Ali, O.M., Abd-Elsalam, K.A., Elkady, F.M. & Hashem, A.H. (2022). Multifunctional silver nanoparticles based on chitosan: antibacterial, antibiofilm, antifungal, antioxidant, and wound-healing activities. *Journal of Fungi*, **8**, 612.
Slinkard, K. & Singleton, V.L. (1977). Total phenol analysis: automation and comparison with manual methods. *American Journal of Enology and Viticulture*, **28**, 49–55.
Soleymanfallah, S., Khoshkhoo, Z., Hosseini, S.E. & Azizi, M.H. (2022). Preparation, physical properties, and evaluation of antioxidant capacity of aqueous grape extract loaded in chitosan-TPP nanoparticles. *Food Science & Nutrition*, **10**, 3272–3281.
Tanaka, T., Onuma, H., Shigihara, T. *et al.* (2019). Anti-osteoporotic effects of syringic acid and vanilic acid in the extracts

of waste beds after mushroom cultivation. *Journal of Bioscience and Bioengineering*, **128**, 622–629.
Tel, G., Apaydin, M., Duru, M.E. & Öztürk, M. (2012). Antioxidant and cholinesterase inhibition activities of three *Tricholoma* species with total phenolic and flavonoid contents: the edible mushrooms from Anatolia. *Food Analytical Methods*, **5**, 495–504.
Thamilarasan, V., Sethuraman, V., Gopinath, K. *et al.* (2018). Single step fabrication of chitosan nanocrystals using *Penaeus semisulcatus*: potential as new insecticides, antimicrobials and plant growth promoters. *Journal of Cluster Science*, **29**, 375–384.
Thu, Z.M., Myo, K.K., Aung, H.T., Clericuzio, M., Armijos, C. & Vidari, G. (2020). Bioactive phytochemical constituents of wild edible mushrooms from Southeast Asia. *Molecules*, **25**, 1972.
Tzeyung, A.S., Md, S., Bhattamisra, S.K. *et al.* (2019). Fabrication, optimization, and evaluation of rotigotine-loaded chitosan nanoparticles for nose-to-brain delivery. *Pharmaceutics*, **11**, 1–17.
Valizadeh, M., Behnamian, M., Dezhsetan, S. & Karimirad, R. (2021). Controlled release of turmeric oil from chitosan nanoparticles extends shelf life of Agaricus bisporus and preserves its postharvest quality. *Food Bioscience*, **44**, 101401.
Yavuz, S. & Gul, U.D. (2022). The use of fungi for the production of biotechnological products in the field of health. *Turk Hijyen ve Deneysel Biyoloji Dergisi*, **79**, 163–172.
Zhang, H., Oh, M., Allen, C. & Kumacheva, E. (2004). Monodisperse chitosan nanoparticles for mucosal drug delivery. *Biomacromolecules*, **5**, 2461–2468.
Zhang, Y., Yang, Y., Tang, K., Hu, X. & Zou, G. (2008). Physicochemical characterization and antioxidant activity of quercetin-loaded chitosan nanoparticles. *Journal of Applied Polymer Science*, **107**, 891–897.

Supporting Information

Additional Supporting Information may be found in the online version of this article:

Figure S1. Chromatogram and calibration curve results of 77 phenolic reference standards screened in the study.

